

Ab initio simulation of a gadolinium-based magnetic resonance imaging contrast agent in aqueous solution

Rodolphe Pollet^{a)}

Laboratoire Francis Perrin, DSM/DRECAM/SPAM-LFP (CEA-CNRS URA2453), Commissariat à l'Énergie Atomique, 91191 Gif-sur-Yvette, France

Dominik Marx

Lehrstuhl für Theoretische Chemie, Ruhr-Universität Bochum, 44780 Bochum, Germany

(Received 11 January 2007; accepted 4 April 2007; published online 8 May 2007)

The first *ab initio* molecular dynamics simulation of a Gd(III)-based contrast agent in explicit aqueous solution at ambient conditions as used in the actual magnetic resonance imaging of human bodies is presented. The description of the structure of this chelate complex is considerably improved with respect to typical force fields and *ab initio* calculations in continuum solvent models if the open 4*f* shell of Gd is included explicitly. The solvation-shell structure is revealed to be anionic and includes a rather short hydrogen bond donated by the hydroxypropyl arm. © 2007 American Institute of Physics. [DOI: 10.1063/1.2736369]

Magnetic resonance imaging (MRI) is a modern noninvasive diagnostic technique commonly used by oncologists to detect brain tumors. Contrast agents (CAs) are often used to enhance the image contrast but they still suffer from low relaxation enhancements; hence high doses of about 0.1 mmol/kg body weight are required. Clinically approved CAs are prevalently gadolinium(III) chelates^{1–3} since Gd³⁺ is highly paramagnetic in view of its seven unpaired 4*f* electrons and has a rather slow electronic relaxation. However, this ion must not be released in the body as such because of its high toxicity so that a biocompatible complexation cage is required. In addition, the chelating ligands must yield a higher affinity for Gd(III) in comparison with other metals commonly present in the human body such as Zn(II), Ca(II), or Cu(II).

Here, we present the first *ab initio* molecular dynamics simulation of one of the commercially available⁴ CAs in ambient water, namely, Gd(HP-DO3A) where HP-DO3A stands for 1,4,7-tris(carboxymethyl)-10-(2'-hydroxypropyl)-1,4,7,10-tetra-azacyclododecane (see Fig. 1 and Ref. 5). Our primary aims are to assess the quality of electronic-structure-based simulations in comparison with experiment, force-field-based approaches, and static *ab initio* calculations, in addition to obtaining reliable insights into the interface between the Gd cage and solvation water, while the long-term goal is to understand the relaxation mechanism.

Car-Parrinello molecular dynamics^{6,7} based on the Perdew-Burke-Ernzerhof (PBE) functional was performed with an in-house modification of the CPMD code^{7,8} which allows for an explicit (spin unrestricted/open-shell) treatment of the 4*f* electrons using a $[1s^2-4d^{10}]$ Gd ultrasoft pseudopotential⁹ with a plane wave cutoff of only 30 Ry in conjunction with a nonlinear core correction;¹⁰ see Ref. 11 for a recent *ab initio* molecular dynamics simulation of a single Gd³⁺ ion in water where the 4*f* electrons were kept in

the core instead. Using our approach, previous PBE calculations¹² have established that structures and energies of microsolvated Gd complexes are obtained with a high accuracy if and only if the 4*f* electrons are part of the valence space, whereas their pseudization leads to errors of $\approx +0.1$ Å and $+10$ – 30 kcal/mol for Gd–O distances and solvation energies, e.g., for $[\text{Gd}(\text{H}_2\text{O})]^{3+}$. Concurrently, similar conclusions were drawn for lanthanide complexes¹³ regarding the at least indirect participation of the *f* electrons in bonding. It is noted in passing that the ultrasoft pseudopotentials employed for O and H provide an excellent description of hydrogen bonding in aqueous systems within the limitations of the functional used.^{14,15} In *ab initio* molecular dynamics simulation, periodic boundary conditions were applied on an ≈ 15.4 Å cubic box containing one Gd(HP-DO3A) complex solvated by 99 water molecules; the system is charge neutral in view of one Gd³⁺ and three carboxylate groups. Nosé-Hoover chain thermostats on nuclei (at 300 K) and electrons ensured adiabatic sampling.^{7,16}

In solution the majority conformer of the octadentate Gd(HP-DO3A) chelate adopts the structure of a square antiprism, as depicted in Fig. 1. The central Gd is kept in between two square planes formed by four nitrogens (blue balls) and four oxygens (red balls), where the oxygen of the flexible hydroxypropyl arm breaks the symmetry in the oxygen hemisphere unlike in Gd(DOTA) with four carboxylates instead. In addition, there is an empty coordination site for a capping water molecule at the pole of the oxygen hemisphere which is known to experience fast exchange.¹⁷ Extensive preequilibration was performed using the GROMACS (Refs. 18 and 19) force field together with standard atomic charges²⁰ and Lennard-Jones parameters.²¹ This was followed by a 1.5 ps relaxation period²² using Car-Parrinello dynamics before computing averages for another 1.6 ps for this system of 355 atoms and 969 valence electrons including seven unpaired 4*f* electrons.

^{a)}Fax: (33)169-081-213; Electronic mail: rodolphe.pollet@cea.fr

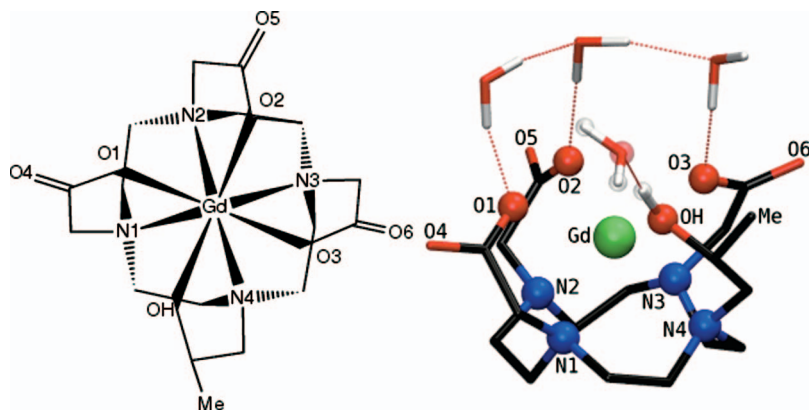


FIG. 1. (Color) Structure of Gd(HP-DO3A): (a) schematic representation and atom numbering and (b) typical snapshot configuration in solution depicting only the four tightly bound water molecules out of 99.

The resulting time-averaged structure characterizing the Gd environment (see Table I) is in excellent agreement with crystallographic data^{23,24} and similar accord is obtained for the dihedrals (not shown). Concerning the overall structure, the chelating nitrogen and oxygen square planes are found to be essentially parallel (average angle $\approx 177^\circ$) and rotated by $\approx 35^\circ$ relative to each other. Previous theoretical investigations^{20,25–27} on similar complexes already concluded that solid-state and solution structures are quite similar, but force field simulations produce Gd–O distances that are systematically too long by $\approx 5\%$, whereas the Gd–N distances are 2%–4% too short,²⁰ if they were not restrained from the outset.^{25,26} Using *ab initio* molecular dynamics simulation the quantitative agreement is much more satisfactory with errors of at most 2%; note that this agreement is expected to deteriorate significantly when including the 4*f* electrons in the pseudopotential core.¹² Furthermore, the Gd binding site is not at all rigid which results in large root-mean-square fluctuations of the Gd–X coordination contacts (see Table I).

Importantly, an accurate description of the local structure around the solvated Gd core is mandatory since it is known to be intimately related to the relaxation process.²⁸ According to the Solomon-Bloembergen-Morgan theory the relaxation rate is governed by a dipole-dipole interaction between the nuclear and electronic spin magnetic moments both assumed to be point dipoles. Thus, the relaxation enhancement required in MRI to improve the image contrast decays like $1/r^6$, where r is the distance between the unpaired electron

spin at Gd and a proton in its solvation shell. A decrease of about 0.2 Å results into a 50% increase in relaxivity¹ which is about the order of magnitude of the change that is introduced, as we showed, when the 4*f* electrons are treated explicitly and not included into the inert pseudopotential core.

Having established the quality of our simulation approach, the next step consists in the investigation of solvation effects. They obviously act differently on the “hydrophilic” (oxygen hemisphere) and “hydrophobic” (macrocycle) faces of the chelate. As a result, the chelating cage is asymmetrically deformed in solution such that the distance between Gd and the oxygen (nitrogen) plane is significantly increased (decreased) with respect to the crystal (see Table I). This inhomogeneous solvation is difficult to reproduce using static *ab initio* calculations of the complex in continuum solvents²⁷ unless it is supplemented by explicit hydrogen bond (HB) interactions.²⁹ Notably, a rather short HB is donated by the hydroxyl group, shaded in Fig. 1(b), with an average O–O distance of only ≈ 2.67 Å and fluctuations down to even 2.33 Å. For such distances, the onset of proton transfer to the attached water molecule can be observed. Furthermore, this particular water molecule features a greatly distorted intramolecular bending angle of about 110° in the average in comparison with $\approx 105^\circ$ for all other water molecules. In comparison with the carboxylate sites, see below, this hydroxypropyl arm is very dynamical, which results for the Gd–OH and Gd–N4 distances into the largest root-mean-square fluctuations (see Table I). With respect to the relaxivity enhancement of Gd(HP-DO3A), the attachment of a water molecule to this hydroxyl group would undoubtedly provide a *second-sphere* mechanism, akin to $[\text{Gd}(\text{DOTP})]^{5-}$ where its four phosphonate groups are strongly hydrogen bonded to solvent molecules.²

Most interestingly, each of those three carboxylate oxygens that are coordinated with Gd preferentially accepts one HB from a close by water molecule. Together with the water molecule bound to the hydroxyl arm, this constitutes the first water shell around the Gd ion beyond the chelate sphere. Typically, at least two out of these three water molecules are themselves linked by additional HBs forming so-called “daisy chains” in an ordered donor-acceptor arrangement. Occasionally these bound water molecules get caught in a network, as depicted in Fig. 1(b), which, together with two additional HBs with water molecules in Gd’s second water

TABLE I. Selected average distances and their root-mean-square fluctuations (in parenthesis) in Å of Gd(HP-DO3A) in ambient water (see text).

	This work	Expt. ^{a,b}
$d(\text{Gd}-\text{O1})$	2.41 (0.08)	2.38
$d(\text{Gd}-\text{O3})$	2.33 (0.07)	2.34
$d(\text{Gd}-\text{O2})$	2.33 (0.07)	2.32
$d(\text{Gd}-\text{OH})$	2.45 (0.09)	2.40
$d(\text{Gd}-\text{N1})$	2.67 (0.09)	2.65
$d(\text{Gd}-\text{N3})$	2.63 (0.07)	2.64
$d(\text{Gd}-\text{N2})$	2.69 (0.08)	2.65
$d(\text{Gd}-\text{N4})$	2.66 (0.10)	2.65
$d(\text{Gd}-\text{O plane})$	0.97 (0.08)	0.75
$d(\text{Gd}-\text{N plane})$	1.56 (0.06)	1.61

^aReference 23.

^bReference 24.

shell (not shown), leads to a locally tetrahedral arrangement with two accepted and two donated HBs similar to bulk water. The hydroxyl-bound water molecule, however, is not involved in hydrogen bonding with respect to the three carboxyl-bound water molecules. This implies that the four closest solvation water molecules do *not* establish a typical cationic solvation sphere around Gd^{3+} but an anionic arrangement with respect to the carboxylates and hydroxypropyl. It is expected that this peculiar HB topology, in conjunction with the flexible hydroxyl arm, will impact on the mechanism that leads to the efficient relaxation enhancement in MRI observed for Gd(HP-DO3A).

In conclusion, we have first of all demonstrated that *ab initio* molecular dynamics simulation of Gd-based contrast agents in explicit aqueous solution, as used in real-life MRI, is feasible. Second, the structural parameters are shown to be improved with respect to typical force fields and *ab initio* calculations using implicit solvent models if the open 4f shell is explicitly included, which is crucial in view of the strong distance dependence of the dipolar image contrast enhancement mechanism. Third, an anionic solvation structure is found at the mouth of the Gd^{3+} gorge, including a very unusual hydrogen bond donated by the hydroxypropyl arm. Last but not the least, by taking into account the electronic structure explicitly, this simulation opens the pathway for the investigation of chemical events that lead to proton exchange phenomena.

The authors wish to thank Nisanth Nair for helpful discussions. This work was partially supported by EMIL Network of Excellence Against Cancer, DFG, and FCI. Computational resources were provided by CCRT at CEA, Bovilab@RUB, and Rechnerverbund-NRW.

¹P. Caravan, J. J. Ellison, T. J. McMurry, and R. B. Lauffer, *Chem. Rev.* (Washington, D.C.) **99**, 2293 (1999).

²S. Aime, M. Botta, and E. Terreno, *Adv. Inorg. Chem.* **57**, 173 (2005).

³P. Caravan, *Chem. Soc. Rev.* **35**, 512 (2006).

⁴M. Bottrill, L. Kwok, and N. J. Long, *Chem. Soc. Rev.* **35**, 557 (2006).

⁵V. M. Runge, D. Y. Gelblum, M. L. Pacetti, F. Carolan, and G. Heard, *Radiology* **177**, 393 (1990).

⁶R. Car and M. Parrinello, *Phys. Rev. Lett.* **55**, 2471 (1985).

⁷D. Marx and J. Hutter, in *Modern Methods and Algorithms of Quantum Chemistry*, edited by J. Grotendorst (NIC, Jülich, 2000), pp. 301–449 (for

downloads see www.theochem.rub.de/go/cprev.html).

⁸J. Hutter *et al.*, CPMD Copyright IBM Corp 1990–2006, Copyright MPI für Festkörperforschung Stuttgart 1997–2001.

⁹D. Vanderbilt, *Phys. Rev. B* **41**, 7892 (1990).

¹⁰S. G. Louie, S. Froyen, and M. L. Cohen, *Phys. Rev. B* **26**, 1738 (1982).

¹¹O. Yazyev and L. Helm, *J. Chem. Phys.* **125**, 054503 (2006).

¹²R. Pollet, C. Clavaguéra, and J.-P. Dognon, *J. Chem. Phys.* **124**, 164103 (2006).

¹³S. Schinzel, M. Bindl, M. Visseaux, and H. Chermette, *J. Phys. Chem. A* **110**, 11324 (2006).

¹⁴B. Meyer, D. Marx, O. Dulub, U. Diebold, M. Kunat, D. Langenberg, and C. Wöll, *Angew. Chem., Int. Ed.* **43**, 6642 (2004).

¹⁵M. E. Tuckerman, A. Chandra, and D. Marx, *Acc. Chem. Res.* **39**, 151 (2006).

¹⁶The wave function cutoff was set to 30 Ry, the fictitious electron mass to 700 a.u., and the target kinetic energy to 0.075 a.u. For the Gd pseudopotential, we have applied minor modifications to our previously published small core ultrasoft pseudopotential (Ref. 12) namely, a reference all electron configuration corresponding to the Gd^{2+} ground state instead of a slightly Gd^{3+} excited state, a unique cutoff radius of 2.0 a.u. for all the angular momentum channels, a cutoff radius of 2.3 a.u. instead of 2.5 a.u. for the local pseudopotential, and a nonlinear core correction (Ref. 10) radius of 0.48 a.u. instead of 0.95 a.u.

¹⁷L. Helm, G. M. Nicolle, and A. E. Merbach, *Adv. Inorg. Chem.* **57**, 327 (2005).

¹⁸H. J. C. Berendsen, D. van der Spoel, and R. van Drunen, *Comput. Phys. Commun.* **91**, 43 (1995).

¹⁹E. Lindahl, B. Hess, and D. van der Spoel, *J. Mol. Model.* **7**, 306 (2001).

²⁰F. Yerly, A. Borel, L. Helm, and A. E. Merbach, *Chem.-Eur. J.* **9**, 5468 (2003).

²¹F. Yerly, K. I. Hardcastle, L. Helm, S. Aime, M. Botta, and A. E. Merbach, *Chem.-Eur. J.* **8**, 1031 (2002).

²²Although the *ab initio* potential energy was relaxed after approximately 1 ps, the relaxation time was set to 1.5 ps to ensure convergence of the integrated absolute value of the spin density ζ (to a value of 7.17), where $\zeta = \int d\mathbf{r} [\rho_\alpha(\mathbf{r}) - \rho_\beta(\mathbf{r})] / \rho(\mathbf{r})$, where ρ_α and ρ_β are the α and β spin densities.

²³K. Kumar, C. A. Chang, L. C. Francesconi, D. D. Dischino, M. F. Malley, J. Z. Gougoutas, and M. F. Tweedle, *Inorg. Chem.* **33**, 3567 (1994).

²⁴Note that in Ref. 23, $d(\text{Gd}-\text{O}3)$ and $d(\text{Gd}-\text{O}7)$, labeled $d(\text{Gd}-\text{O}2)$ and $d(\text{Gd}-\text{O}H)$ in the present paper, as well as $d(\text{Gd}-\text{N}2)$ and $d(\text{Gd}-\text{N}4)$ are interchanged in Table 6, while the Cartesian coordinates in Table 4 are correct.

²⁵R. J. Dimelow, N. A. Burton, and I. H. Hillier, *Phys. Chem. Chem. Phys.* **9**, 1318 (2007).

²⁶E. S. Henriques, C. F. G. C. Geraldés, and M. J. Ramos, *Mol. Phys.* **101**, 2319 (2003).

²⁷U. Cosentino, A. Villa, D. Pitea, G. Moro, V. Barone, and A. Maiocchi, *J. Am. Chem. Soc.* **124**, 4901 (2002).

²⁸I. Solomon, *Phys. Rev.* **99**, 559 (1955).

²⁹C. P. Kelly, C. J. Cramer, and D. G. Truhlar, *J. Phys. Chem. A* **110**, 2493 (2006).